PROCEEDINGS OF SCIENCE

Investigating In-Medium Effects with FOPI Spectrometer

Victoria Zinyuk* **for the FOPI Collaboration** †
Physikalisches Institut der Universitat Heidelberg, Heidelberg, Germany
E-mail: V.Zinyuk@gsi.de

Hadron properties are expected to be modified in dense baryonic matter. Strange particles produced sub- or close-to-production threshold energies allow to probe a possible modification. In this review we report on the status of FOPI's investigation of In-Medium Effects at normal nuclear matter density in pion-induced reactions and at 2-3 ρ_0 in heavy ion reactions.

International Winter Meeting on Nuclear Physics,
21-25 January 2013
Bormio, Italy

*Speaker.
†Supported by BMBF 05P12VHFC7

PoS(Bormio 2013)066

1. Introduction

In-Medium Effects

Hadrons are believed to undergo modifications of their properties, in hot and dense baryonic matter. Modification of properties such as production cross sections, width or mass may influence the production and propagation of hadrons in nuclear medium. Various theoretical approaches agree qualitatively in predicting density dependent changes in mass and coupling constants for kaons and anti-kaons, resulting in the growth(drop) of the effective mass of kaons(anti-kaons) with increasing nuclear matter density [1]. These modifications are parametrized as a density dependent mean field $KN(\bar{K}N)$-potential, repelling(attracting) the kaons(anti-kaons) toward nucleons.

Enormous effort was invested to deduce the strength of the KN- and $\bar{K}N$-potentials. The main results are summarized in Table 1. Clear evidence was found that kaons collectively propagate in the opposite direction to that of protons [2] [3], which is compatible with the idea of repulsion. In order to draw any quantitative conclusion on the depth of the potential various effects(e.g. scattering, absorption) have to be take into account which is only possible in microscopic transport calculations, modeling the dynamical evolution of the HIC.

observable	U(KN)[MeV] @ $\rho = \rho_0$	U($\bar{K}$N)[MeV] @ $\rho = \rho_0$	measured by
charged kaons:			
K^+ yield (cent)	model-dep.	–	FOPI(1997) [4]
K^+ sideflow, v_1 (cent)	20 (HSD)	–	FOPI(2000) [2]
$K^\pm$ v_1 (per)	0 (IQMD)	- 45 (IQMD)	FOPI(2013)[3]
$K^\pm$ v_1 (per)	0 (HSD)	- 25 (HSD)	FOPI(2013) [3]
K^-/K^+-ratio	30 (RBUU)	- 70(RBUU)	FOPI(2000) [5]
K^+- *ratio heavy/light sys.**	20 (HSD)		ANKE(2004) [6]
neutral kaons:			
K^0_S- $p_t$spectra	40 (IQMD)	–	HADES(2010) [7]
K^0_S- yield	0 (IQMD)	–	FOPI(2004) [8]
K^0_S- inverse slope	20 (IQMD)	–	FOPI(2004)[8]
K^0_S- *ratio heavy/light sys.**	20 (HSD)	–	FOPI(2009) [9]

Table 1: Summery of the recently available measurement of $KN(\bar{K}N)$-potential.
* *elementary reactions*

In this report we discuss two different observables:

1. The collective flow [10] of K^+ and K^--mesons in Ni+Ni at 1.9 AGeV.

At this beam energy kaons are produced close-to-production threshold and anti-kaons sub-production threshold energies which makes them highly sensitive to a possible repulsion/attraction in baryonic matter.

This measurement allows to investigate the IME at 2-3 ρ_0 and at temperature around 100 MeV in a wide rage of the impact parameter [11] [12].

Experimental findings are compared to Hadron String Dynamics (HSD) model [13] and Isospin

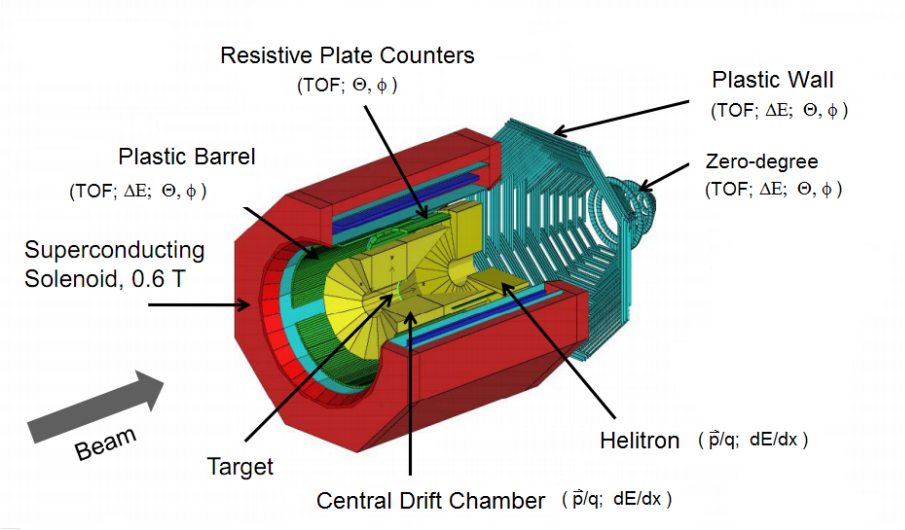

Figure 1: The FOPI Detector in Phase II.

Quantum Molecular Dynamics (IQMD) [14]. In HSD a KN - potential of 20 ± 5 MeV and in IQMD of 40 ± 5 MeV for particles at rest ($p = 0$), at normal nuclear matter density and a linear baryon density dependence is employed. The momentum dependence of the KN - potential is of minor importance, because the produced kaons have only a very small relative momentum with respect to the medium and therefore also the influence from the momentum dpenedence is expected to be small. This effect has been omitted in the transport calculations (compare [15]). A similar, but attractive potential is used in IQMD as K^-N - potential with $U_{K^-N}(\rho = \rho_0, p = 0) = -90$ MeV and a G-Matrix formalism corresponding to $U_{K^-N}(\rho = \rho_0, p = 0) = -50$ MeV is employed in HSD [16].

2. 'Momentum ratios' in pion-induced reaction, i.e. differences in population of the phase space in the final state for kaons produced in heavy and light targets.

The beam momentum of 1.7 GeV/c was chosen such that the direct production of K^+K^--pairs is possible. Thereby recorded sample of charged kaons, produced close to threshold, is highly sensitive to the $KN(\bar{K}N)$-potential and allows to study in-medium effects at normal nuclear matter density.

The FOPI Detector and PID

The FOPI spectrometer is a large acceptance detector system located at the SIS-18 accelerator at GSI, Darmstadt, Germany [17]. (Fig. 1). The core part of the detector is the Central Drift Chamber(CDC) placed inside a superconducting solenoid. The CDC covers $33^\circ < \Theta_{lab} < 131^\circ$ [a] and provides information about the energy loss and track of a particle. By correlating the energy loss and the momentum - deduced from the curvature in the magnetic field - a mass measurement and therefore a particle identification is possible. The drift chamber is surrounded by a time-of-flight system which provides additional information about the velocity of a particle and allows for a second mass identification.

[a] with respect to nominal target position

To improve the kaon identification capability, the FOPI detector was upgraded with a new time-of-flight barrel covering the polar angle range $37^\circ < \Theta_{lab} < 68^\circ$ [a] based on Multistrip-Multigap-Resistiv-Plate Counters(MMRPC)[18]. In the polar angle range $68^\circ < \Theta_{lab} < 132^\circ$ [a] a plastic scintillator barrel is used for velocity measurements.
In the MMRPC - acceptance the overall time resolution is 88 ps, in which the MMRPC time resolution is σ_{MMRPC} = 65 ps. With this time resolution charged kaons can be identified up to $p_{K^+/K^-} = 1$ GeV/c without significant contamination from fast pions.

In the forward direction, $\Theta_{lab} < 30^\circ$ [a], the detector is completed by another drift chamber the 'Helitron' and a ToF-detector the 'Plastic Wall', which allows an almost full solid angle coverage in the laboratory frame.

Neutral particles are identified by their decay products, e.g. the K^0_S-mesons are measured as a peak in the invariant mass of π^+ and π^- (branching ratio BR=69 %) around the nominal kaon mass.

2. Azimuthal Anisotropies

Anisotropies in the azimuthal emission pattern can be quantified by expressing the azimuthal distribution in a Fourier series:

$$\frac{dN}{d\phi} \propto (1 + 2v_1 cos(\phi) + 2v_2 cos(2\phi) + ...), \tag{2.1}$$

with ϕ the azimuthal angle of the outgoing particle with respect to the reaction plane [19]. The reaction plane is reconstructed event-wise by the transverse momentum method [20]. The first order Fourier coefficient, v_1, describes the collective sideward deflection of particles in the reaction plane, called 'directed flow'. The second order Fourier coefficient, v_2, describes the emission probability in - versus out- of the reaction plane, referred to as 'elliptic flow' [21, 2]. The Fourier coefficients are corrected for the accuracy of the reaction plane determination (eventwise) according to the Ollitrault method [22]. The mean correction values, which reflect the accuracy of the reaction plane determination, are given in Table 2. Note that peripheral events (Mul < 20) were rejected to assure a minimal accuracy of the reaction plane determination.

Results

The experimental data on v_1 and v_2 of $K^\pm$ for the overall event sample (a) (see Table 2) are presented as function of nomalized rapidity $y_{(0)} = y_{lab}/y_{cm} - 1$ in Fig. 2.

Around the target rapidity K^+'s are collectively deflected in-plane in the direction opposed to that of protons (Fig. 2 (a)). Additionally the K^+ - mesons are observed to collectively move out-of-plane (Fig. 2 (c)) as indicated by the negative v_2 values. K^- - mesons (Fig. 2 (b) and (d)), show an isotropic emission, both in- and out-of-plane, i.e. v_1 and v_2 are compatible with zero within the sensitivity of the data.

To link the measurements to the depth of the $KN(\bar{K}N)$-potential we compare the measurements to the transport model prediction of HSD and IQMD depicted by the full lines in Fig. 2.
According to the models the largest sensitivity to the presence of in-medium potentials is achieved

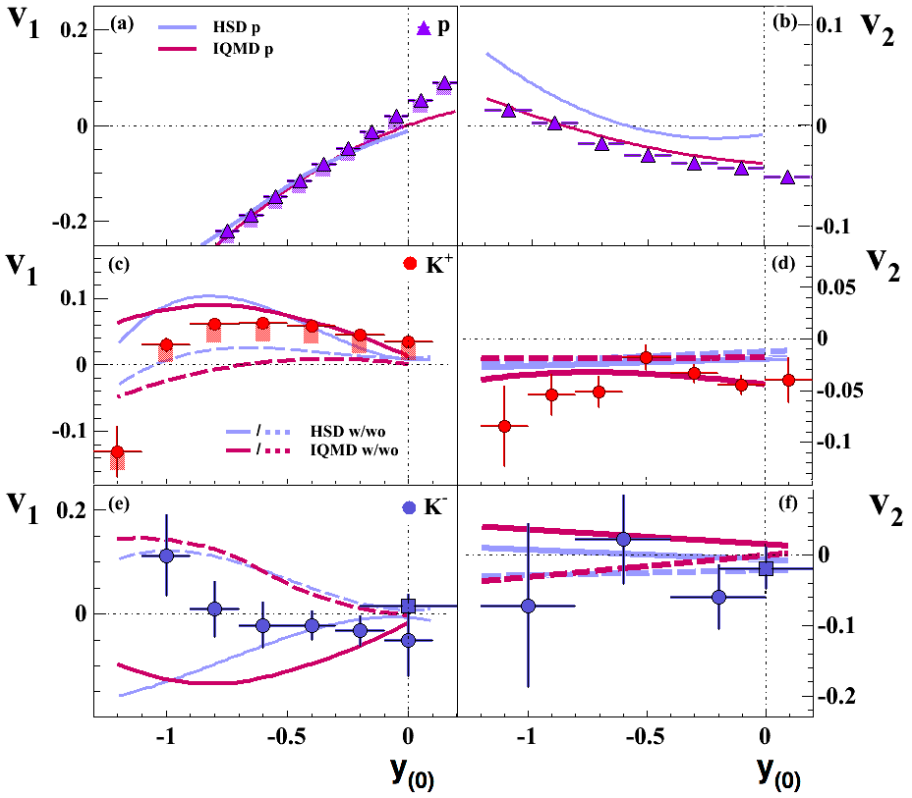

Figure 2: First and second Fourier Coefficients v_1 and v_2 as a funciton of normalized rapidity for protons (panels (a) and (b)), K^+-mesons (panels (c) and (d)) and K^--mesons (panels (e) and (f)) compared to the prediction of HSD(lilac) and IQMD(pink) trasport models with (solid lines) and without(dashed lines) the assumption of KN-potential. Error bars(boxes) denote the statistical(systematic) uncertainties. Note: Model calculations without in-medium potential (dashed lines) still include $K^+N(K^-N)$ rescattering and absorption processes for K^- [3].

with the sideflow observable v_1 at backward rapidities. Without in-medium modifications the K^+ - mesons are emitted isotropically, i.e. v_1 and v_2 values are close to zero. The repulsive K^+N - potential pushes the K^+ - mesons away from the protons, thus generating the 'antiflow' of K^+ - mesons. The magnitude of the 'antiflow' is, however, not correctly described by the models. For K^- - meson the interpretation is different: due to the strong absorption by strangeness exchange reactions with baryons, an 'antiflow' signature is expected without the presence of a potential (Fig. 2 (b)). An attractive K^-N - potential is clearly necessary to explain the observed v_1 - values. The default potential employed in HSD and IQMD predicts a much stronger effect than experimentally observed, indicating that the K^-N - potential is weaker than the default parametrization.
Note: For all HSD and IQMD prediction with and without in-medium modifications absorption and rescattering are taken into account by the transport calculations.

The second harmonic v_2 of K^+ (Fig. 2 (d)) shows a squeeze-out signature at midrapidity which is describes within IQMD by a presence of a KN-potential and not reproduced by HSD. Note that also the amount of the out-of-plane emission of protons (Fig. 2 (b)) is underestimated by HSD for the considered reaction. In case of K^- (Fig. 2 (f)) no conclusions about the presence of an

	Mul	σ [b]	$\langle b \rangle \pm \Delta b$ [fm]	f_1	f_2
(a)	[20,90]	1.09 ± 0.1	3.90 ± 1.41	1.5 ± 0.1	3.0 ± 0.1
(p)	[20,48]	0.79 ± 0.05	4.54 ± 0.95	1.5 ± 0.1	3.0 ± 0.1
(c)	[49,90]	0.3 ± 0.05	2.11 ± 0.80	1.6 ± 0.1	3.1 ± 0.2

Table 2: Definition of event classes: (a) total, (p) peripheral and (c) central events. The baryon multiplicity Mul contains all charged particles from the Plastic Wall ($6.5^\circ < \theta_{lab} < 23^\circ$) and p, d, t, ^3He and α from the CDC. The corresponding cross section σ, mean impact parameter $\langle b \rangle$, the RMS of $\langle b \rangle$: Δb and the reaction plane correction factors f_1 for v_1 and f_2 for v_2 are listed. Centrality selection, imposed on the data, is realized by weighting the events with an impact parameter dependent function, that is obtained by evaluating the influence of the multiplicity selection on the impact parameter distribution within the IQMD model [14] that describes the multiplicity distribution reasonably well.

in-medium potential can be drawn from this observable with statistic sensitivity of the data.

To further investigate the discrepancy of the HSD predictions with the data shown in Fig. 2 we evaluate in Fig. 3 the dependence of v_1 on the transverse momentum p_T for K^+ - mesons near target rapidity ($-1.3 < y_{(0)} < -0.5$) for the two centrality classes (p) and (c) defined in Table 2. The data shows a strong p_T dependence. The values of v_1 are observed to drop with increasing momentum. Near threshold beam energies, the major part of kaons is produced with small momenta. The kaons gain momentum by rescattering with energetic nucleons and therefore their flow strength increases in the direction of nucleons [23]. The v_1 values of protons are negative (Fig. 2 (a)) and therefore the v_1 values of K^+ decrease with increasing momentum. Additionally, at low p_T's, the larger density gradient in peripheral collisions causes stronger in-plane deflection of kaons from peripheral compared to that from central events . In the central event sample the data is described by the HSD calculation with $U_{K^+N} = 20$ MeV in agreement with the previous FOPI data [2]. In the peripheral event sample, HSD overestimates the magnitude of v_1 especially at low p_T. IQMD does not reproduce the p_T-dependence of v_1 observed in the data.

3. Ratio of Momentum Distribution

The Observable

Elementary reactions allow to study the KN - potential at normal nuclear matter density. In pion-induced reactions strange mesons can be directly produced at relativly low beam energy (compared to other elementary reactions). In π-induced reactions with a heavy target K-mesons are produced on the surface of the nucleus (for considered beam energies) and have to propagate through the nucleus to be detected. If the kaon feels a $KN(\bar{K}N)$- potential, i.e. is attracted(repelled) by the nuclear matter, its momentum distribution in the final state will be shifted to smaller(larger) momenta. These changes in the phase space distribution can be quantified by comparing the momentum spectra of kaons produced in a heavy target to a reference system provided by a light target, as illustrated in Fig. 4. Note: In a HIC no difference between heavy and light target would be visible, due to equilibration by scattering processes in both systems.
Scattering and absorption inside the nuclei influence the momentum distribution in the final state. Particles like K^+- and K^0_S-mesons have a large mean free path (compared to the size of the consid-

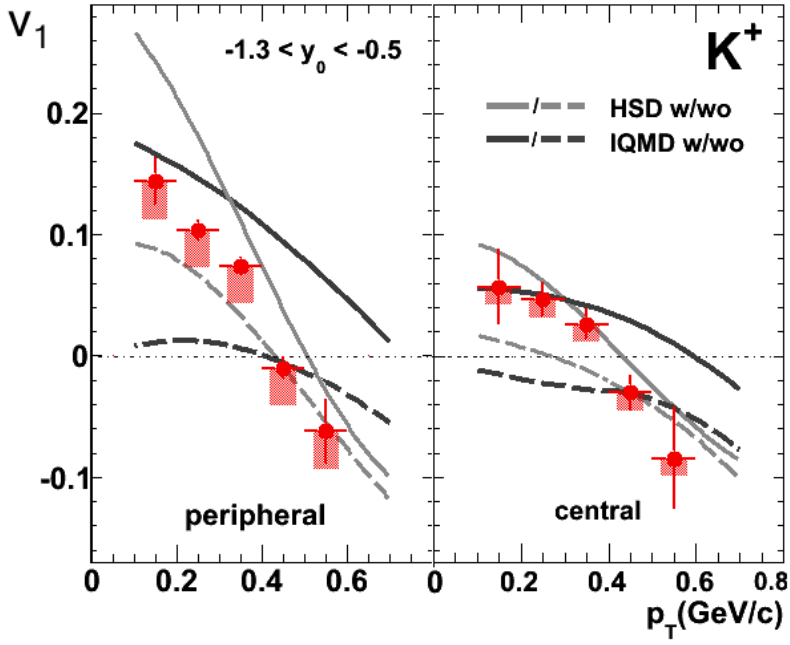

Figure 3: First Fourier Coefficient as a funciton of transverse momentum in the near-target rapidity for K^+-mesons *Left:* Peripheral event selection *Right:* Semi-central event selection (see Table 1) The data is compared to HSD(grey) and IQMD(black) transport approaches with(solid lines) and without(dashed lines) the assumption of a K^+N-potential. [3]

ered systems), here the effect from a potential is expected to be influenced only weakly. Particle like K^--mesons and Λ-baryons on the other hand have a very small mean free path in nuclear matter, they are expected to be strongly absorbed. This could mean that the major part of the measured particles have been produced in the secondary collisions close to the surface of the nucleus and do not feel the potential. However the recent version of HSD predictions for K^-, taking into account scattering and the effect from repulsive $\bar{K}N$-potential, shows a clear effect from the potential.

The Momentum Ratios for K-mesons

First results, from a recent experiment, of such momentum ratios $R((dN/dp)_{Pb}/(dN/dp)_C)$ are presented in Fig. 5 for K^0_S-mesons and in Fig. 6 for K^+-mesons (left panel), K^--mesons (right panel). In case of K^+-mesons repulsion from nuclear matter due to strong interaction(the KN-potential), and an additional repulsion due to the Coulomb-interaction are observed. Therefore, the low momentum region of the phase space of K^+-mesons from the heavy target is populated weaker than the one from the reference system, i.e. light target. The ratio of the momentum distributions has small values and rises as the momentum increases. Particles with larger momentum leave the interaction region rapidly and therefore are not influenced by the repulsion. The phase space distributions in both systems are equal and the momentum ratio reaches a constant value.
The discussed effects from the strong interaction has been observed in earlier measurements by the FOPI Collaboration for K^0_S [9] and the interplay of strong and Coulomb interactions for K^+-mesons by the ANKE collaboration [6] Fig. 5(upper right). Transport model calculations confirm the expectations for different scenarios. K^+ and K^0_S were found to be good probes for in-medium effects

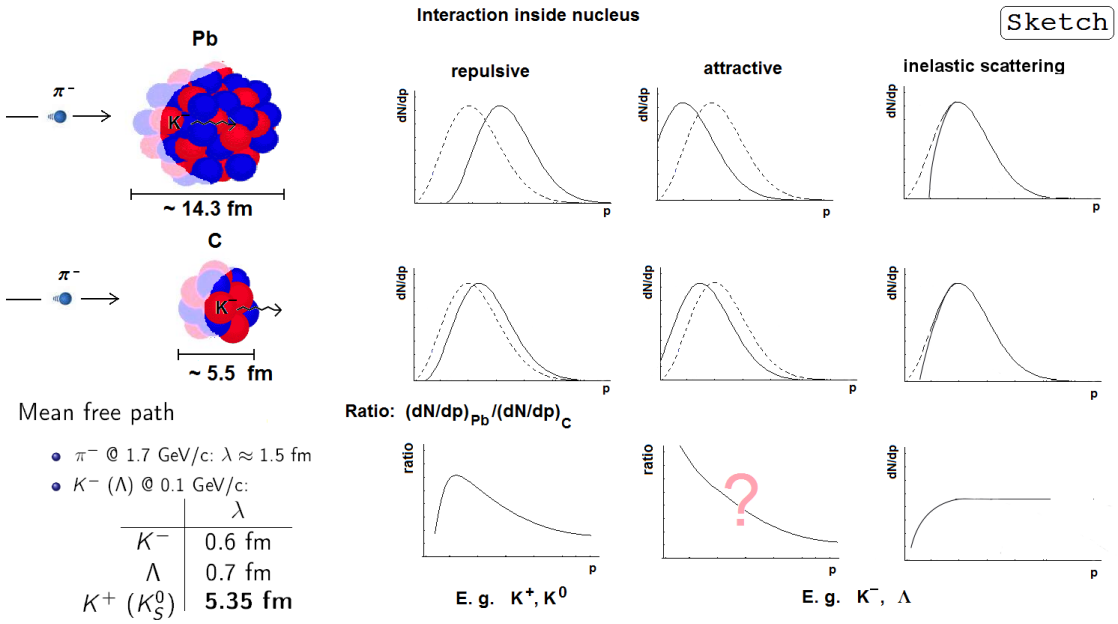

Figure 4: The 'Momentum Ratio' observable. Sketch of the expectations for the ratio of strange particles produced in a heavy target to the one produced in a light target for different scenarios of the interaction inside nuclear matter.

due to relatively long mean free path in nuclear matter at small momenta. Our new measurement is in qualitative agreement with the previous one (Fig. 5). The momenta with the highest ratio and the region with a constant ratio are compatible to the ANKE results, however the strong decrease, measured before at smaller momenta, is not observed.

In case of the attracted particles, like K^-, one would expect the largest value for the momentum ratio at smallest momentum and a continuous decrease with increasing momenta, as far as the $\bar{K}N$-potential is concerned. On the other hand, K^--mesons have a very short mean free path in nuclear matter of about 0.6 fm for $p_{K^-} = 0.1 GeV/c$ and therefore they are expected to suffer collisions in both heavy and light targets. Part of K^--mesons are absorbed in inelastic scattering processes another part exchanges momentum as a consequence of elastic scattering. Both processes influence the momentum distribution in the final state. Our recent measurement (Fig. 6, right) suggest that K^--mesons with small momenta are absorbed in the heavier system to a larger fraction than in the light one. Note: This behavior is not reproduced by transport calculations yet. K^--mesons with $p_{K^-} > 0.3$ GeV/c behave equally in the heavy and light systems, i.e. the momentum ration is constant.

4. Summery

Understanding of the interaction of K-mesons with nuclear matter is far from complete. The sideflow observable v_1 of kaons and antikaons produced close to the threshold energies shows sensitivity to the influence form the $KN(\bar{K}N)$-potential. Evidences for a repulsive KN-potential and a weakly attractive $\bar{K}N$-potential are found in comparison to transport model calculation. However the theoretic modeling is far from satisfactory as is demonstrated by the detailed comparison of the

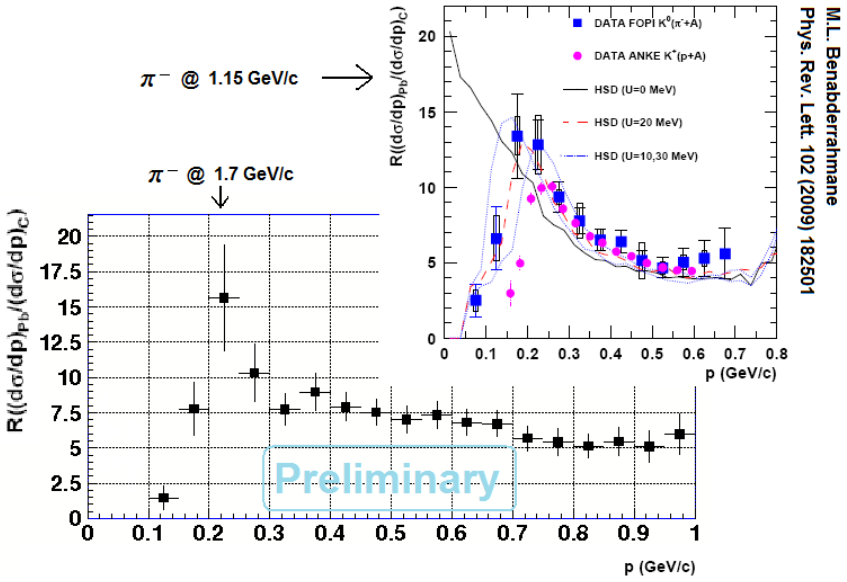

Figure 5: 'Momentum Ratio' for K^0_S-mesons measured in pion-induced reactions for beam momentum of 1.15 GeV/c (*upper right*) and beam momentum of 1.7 GeV/c.

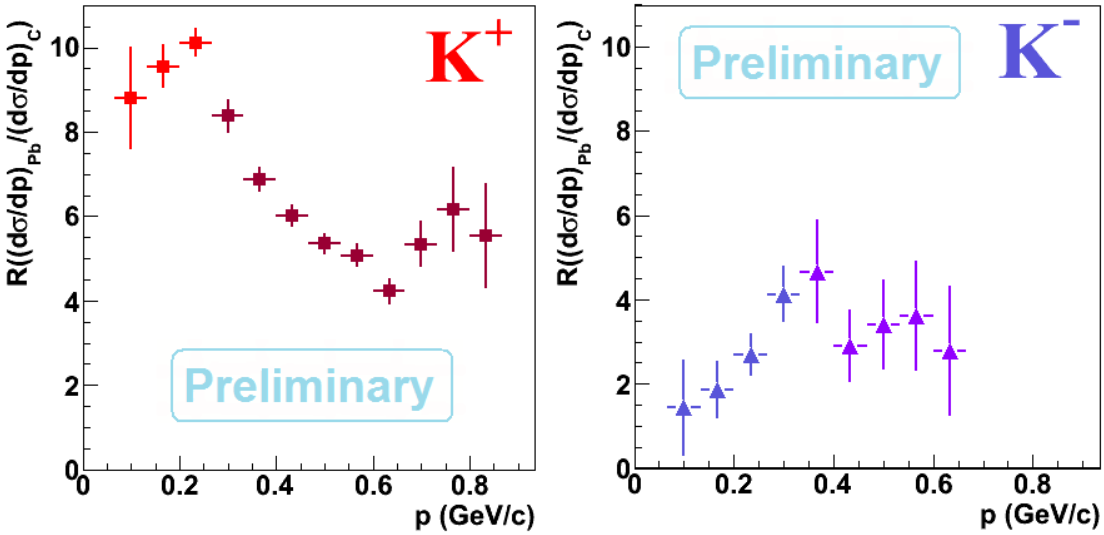

Figure 6: Ratio of momentum distributions of charged kaons produced in a heavy target to light target. Note: Different colors indicate a separate analysis of different detector components.

differential flow pattern of the K^+ - mesons.

At normal nuclear matter density the 'Momentum Ratio' observable can be used to characterize the differences in the phase space population caused by the presence of in-medium interactions The results of the recent analysis are consistent with the previous measurement. However to deduce the influence of the potential further investigation – in cooperation with transport theories – are intended.

References

[1] D.B. Kaplan and A.E. Nelson, Phys. Lett. B **175**, 57 (1986);G.E. Brown and M. Rho,Phys. Rev. Lett. **66**, (1991) 2720;G.Q. Li and C.M. Ko,Phys. Lett. B **338**, (1994) 118; M. Lutz, Phys. Lett. B **426**, 12 (1998); Nucl. Phys. A **574**, 755 (1994);T. Waas, N. Kaiser and W. Weise,Phys. Lett. B **379**, 34 (1996); **365**, 12 (1996).

[2] P. Crochet *et al.*, Phys. Lett. B **486**, 6 (2000).

[3] T. Kang, V. Zinyuk *et al.*, to be published.

[4] D. Best *et al*., Nucl. Phys. A **625**, 307 (1997); F. Laue *et al*., Phys. Rev. C **82**, 1460 (1999).; M. Menzel *et al.*, Phys. Lett. B**495** (2000) 26-32

[5] K. Wisniewski *et al*., Eur. Phys. J. A **9**, 515 (2000).

[6] M. Bueschner *et al*., Eur. Phys. J. A **22**, 301 (2004).

[7] HADES Collaboration, Phys. Rev. C**82** (2010) 044907

[8] M. Merschmeyer, Ph. D. thesis, Ruperto-Carola University of Heidelberg

[9] M.L. Benabderrahmane *et al.*, Phys. Rev. Lett. **102**, 182501 (2009).

[10] N. Herrmann *et al.*,Ann. Rev. Nucl. Part. Sci. **49**, 581 (1999); W. Reisdorf and H.G. Ritter *et al.*, Ann. Rev. Nucl. Part. Sci. **47**, 663 (1997).

[11] C. Fuchs,Prog. Part. Nucl. Phys. **56**, 1 (2006).

[12] B. Hong *et al.*, Phys. Rev. C **57**, 244 (1998).

[13] W. Cassing *et al.*, Phys. Rep. **308**, 65 (1999)

[14] C. Hartnack *et al.*, Eur. Phys. J. A 1, 151 (1998)

[15] C. Hartnack *et al.*, Phys.Rep. **510**, 119 (2012)

[16] W. Cassing *et al.*, Nucl. Phys. A **727**, 59 (2003).

[17] A. Gobbi *et al.* Nucl. Instr. Meth. A **324**, 156 (1993);J. Ritman *et al.*,Nucl. Phys. B, Proc., Suppl. **44**, 708 (1995).

[18] M. Kiš *et al.*, Nucl. Instr. and Meth. A **646**, 27 (2011);

[19] S. Voloshin and Y. Zhang, Z. Phys. C **70**, 665 (1996).

[20] P.Danielewicz, G.Odyniec, Phys. Lett. **157B**, 146 (1985).

[21] A. Andronic *et al.*, Phys. Lett. B **612**, 173 (2005).

[22] Jean-Yves Ollitrault,Nucl. Phys. A **638**, 195c (1998)

[23] G.Q. Li and G.E. Brown, Nucl. Phys. A **636**, 487 (1998).